Chapter 8

Condensation Inside Tubes

(Revised in 2006)

SUMMARY: The principles of condensation in horizontal tubes are reviewed. The effect of flow regimes and flow stratification are shown to be important in predicting local condensation heat transfer coefficients. In addition to condensation in plain tubes, condensation in microfin tubes and condensation of zeotropic mixtures are also addressed along with condensation of superheated vapor and the subcooling of condensate.

8.1 Condensation inside Horizontal Tubes

This chapter covers condensation inside tubes. Presently, only condensation inside *horizontal* tubes is reviewed here. The condensation of both pure vapors and condensable mixtures is covered.

Condensation in horizontal tubes may involve partial or total condensation of the vapor. Depending on the application, the inlet vapor may be superheated, equal to 1.0 or below 1.0. Hence, the condensation process path may first begin with a dry wall desuperheating zone, followed by a wet wall desuperheating zone, then a saturated condensing zone and finally a liquid subcooling zone. The condensing heat transfer coefficient is a strong function of local vapor quality, increasing as the vapor quality increases. The condensing heat transfer coefficient is also a strong function of mass velocity, increasing as the mass velocity increases. Opposed to external condensation, intube condensation is independent of the wall temperature difference (T_{sat}-T_w) for most operating conditions, except at low mass flow rates.

8.1.1 Flow Regimes for Condensation in Horizontal Tubes

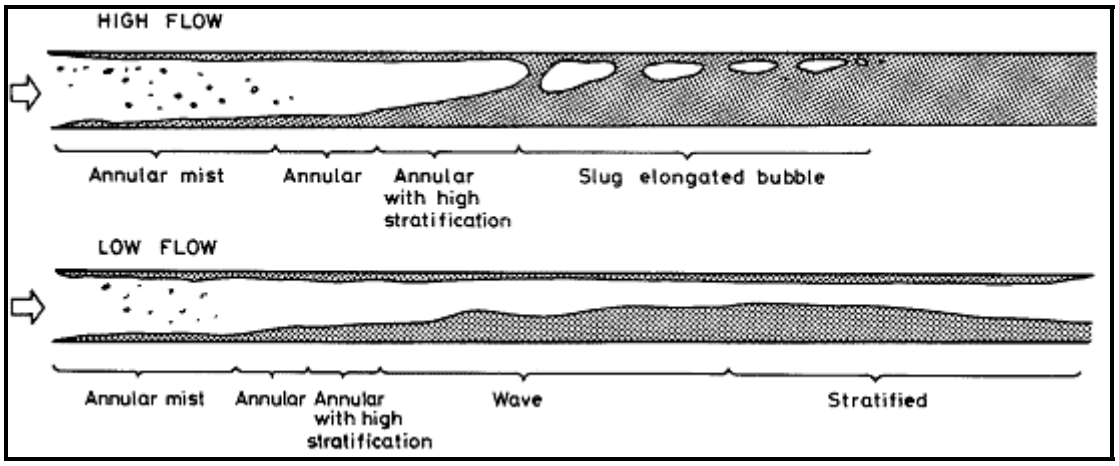

Figure 8.1. Typical flow patterns encountered for condensation inside horizontal tubes.

Figure 8.1 from Palen, Breber and Taborek (1979) illustrates the two-phase flow patterns typical of condensation in horizontal tubes. In the top diagram at high mass flow rates, the flow takes on the annular flow regime, where the liquid film is on the perimeter of the wall, the vapor is in the central core and some liquid is entrained in the vapor from the tips of waves on the interface of the film. As condensation

proceeds along the tube, the vapor velocity decreases and thus there is a corresponding decrease in vapor shear on the interface and the liquid film becomes thicker at the bottom of the tube than at the top. New condensate formed adds to the thickness of the liquid film. As the quantity of liquid increases along the tube, slug flow is encountered and still further along all the vapor is finally converted to liquid. At low flow rates depicted in the lower diagram, at the entrance region annular flow is formed but this quickly transforms to intermittent flow with its characteristic large amplitude waves washing the top of the tube or to stratified-wavy flow with smaller amplitude waves. If liquid does not span the cross-section of the tube, vapor may reach the end of the tube without condensing.

There is a great similarity between these flow regimes and those for adiabatic two-phase flows. Here, however, condensate forms all around the tube perimeter even in stratified flows. As illustrated in Figure 8.2, the fully stratified flow regime with all the liquid normally in the lower portion of the tube for adiabatic flow will have a thin layer of condensate around the upper perimeter.

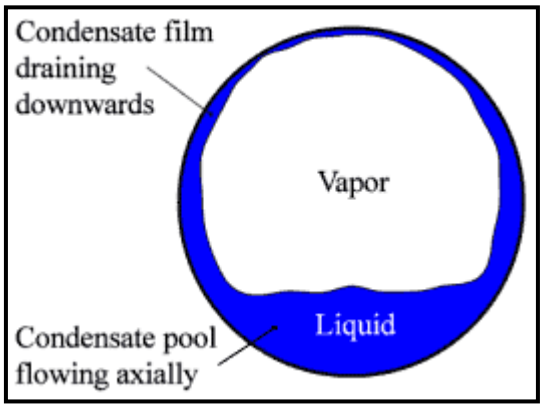

Figure 8.2. Condensation in fully stratified flow.

8.1.2 Condensation of Pure Vapor in a Horizontal Tube

As illustrated in Figure 8.3, at low flow rates the flow is stratified. There is a film of condensate formed by film-wise condensation that drains from the top of the tube towards the bottom under the force of gravity. The film flow is laminar and primarily downwards when the vapor core velocity is low. If the vapor shear is sufficient and the onset to turbulence has been surpassed, then a turbulent film is formed whose predominant flow direction is axial.

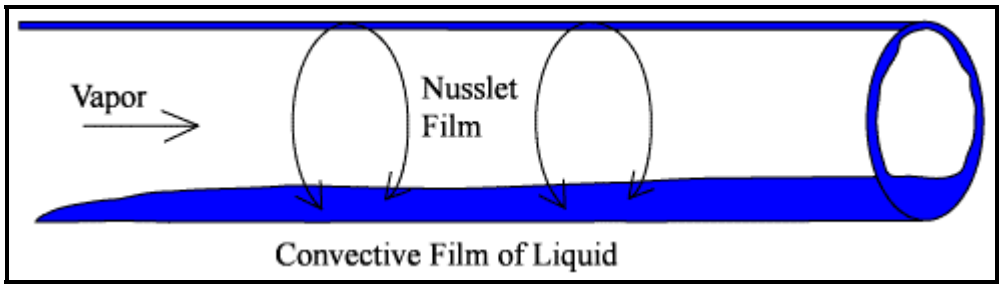

Figure 8.3. Stratified flow with film condensation around the top internal perimeter of the tube.

For low vapor shear conditions, the condensation process on the *inside* perimeter around the top and sides of the tube is very similar to that on the *outside* of a horizontal tube. Thus, Nusselt falling film analysis may be applied to the upper zone of the tube, which has been done first by Chaddock (1957) and then by Chato (1962). The cross-sectional area of the stratified liquid layer at the bottom of the tube can be established from the local void fraction ε. Then, the stratified liquid angle θ_{strat} is can be determined from geometry. The local heat transfer coefficient at this vapor quality x is obtained by proration of the respective heat transfer coefficients with respect to the fraction of the perimeter they occupy as

$$\alpha(x) = \frac{\theta_{strat}}{\pi}\alpha_f + \frac{\pi - \theta_{strat}}{\pi}\alpha_{strat} \qquad [8.1.1]$$

θ_{strat} is the angle from the top of the tube to the stratified layer and is thus equal to π when there is no stratified layer present. θ_{strat} is expressed in radians. α_f is the mean heat transfer coefficient for the film obtained by integration of [7.5.11] from 0 to $(\pi-\theta_{strat})/2$. The heat transfer coefficient for the stratified flow in the bottom of the tube is α_{strat}. Assuming that α_{strat} is negligible compared to α_f, the second term can be neglected while α_f is determined as:

$$\alpha_f = \Omega\left[\frac{\rho_L(\rho_L-\rho_G)gk_L^3 h_{LG}}{\mu_L d_i(T_{sat}-T_w)}\right]^{1/4} \qquad [8.1.2]$$

The value of Ω is a geometric function of θ_{strat} where $\Omega = \beta\theta_{strat}/\pi$ and k_L is the liquid thermal conductivity. Jaster and Kosky (1976) have shown that the value of Ω is related to the vapor void fraction ε as $\Omega = 0.728\varepsilon$. They used the Zivi (1964) void fraction equation, which is a function of vapor quality x and the vapor and liquid densities:

$$\varepsilon = \frac{1}{1+[(1-x)/x](\rho_G/\rho_L)^{2/3}} \qquad [8.1.3]$$

At higher flow rates where turbulent annular flow conditions are confronted, numerous correlations have been proposed: Akers, Deans and Crosser (1959), Cavallini and Zecchin (1974), Shah (1979), etc. Akers, Deans and Crosser proposed a modified version of the Dittus-Boelter (1930) single-phase turbulent tube flow correlation, developed with a database for several refrigerants and organic fluids. Their local condensing coefficient is

$$\frac{\alpha(x)\,d_i}{k_L} = C\,Re_e^n\,Pr_L^{1/3} \qquad [8.1.4]$$

The equivalent Reynolds number for two-phase flow Re_e is determined from an equivalent mass velocity, which in turn is obtained by applying a multiplying factor to the total mass velocity:

$$\dot{m}_e = \dot{m}\left[(1-x)+x\left(\frac{\rho_L}{\rho_G}\right)^{1/2}\right] \qquad [8.1.5]$$

The total mass flow rate of liquid plus vapor is used for the total mass velocity. The empirical parameters C and n to use in [8.1.4] are:

C = 0.0265 and n = 0.8 for $Re_e > 50{,}000$

C = 5.03 and n = 1/3 for $Re_e < 50{,}000$

With the Dittus-Boelter correlation as a starting point, Shah (1979) proposed an alternative multiplier (see brackets) acting on the liquid Reynolds number as

$$\frac{\alpha(x)\,d_i}{k_L} = 0.023\,Re_L^{0.8}\,Pr_L^{0.4}\left[(1-x)^{0.8}+\frac{3.8x^{0.76}(1-x)^{0.04}}{p_r^{0.38}}\right] \qquad [8.1.6]$$

He used the reduced pressure p_r ($p_r = p_{sat}/p_{crit}$ where p_{sat} is the saturation pressure and p_{crit} in the critical pressure of the fluid) rather than the density ratio and a database for condensation of steam, refrigerants and organic fluids. Re_L is the tubular liquid Reynolds number determined with the total mass flow rate of liquid plus vapor.

Thome (1994b, 1998) recommended using the Shah correlation when mass velocities are greater than 200 kg/m^{2}s and that of Akers, Deans and Crosser (1959) when they are lower, based on comparisons to local test data in the literature for R-134a, R-22 and others.

Dobson and Chato (1998) have proposed a vast improvement of the Chato (1962) method that includes both a stratified-wavy flow method with film condensation from the top towards the bottom of the tube and an annular flow correlation. Their annular flow condensation correlation is

$$Nu(x) = 0.023\,Re_{Ls}^{0.8}\;Pr_L^{0.4}\left[1+\frac{2.22}{X_{tt}^{0.89}}\right] \qquad [8.1.7]$$

where the local Nusselt number Nu(x) is based on the tube diameter d_i as

$$Nu(x) = \frac{\alpha(x)\,d_i}{k_L} \qquad [8.1.8]$$

Their superficial liquid Reynolds number Re_{Ls} is

$$Re_{Ls} = \frac{\dot{m}\,d_i\,(1-x)}{\mu_L} \qquad [8.1.9]$$

The Martinelli parameter for turbulent flow in both phases, X_{tt}, is

$$X_{tt} = \left(\frac{1-x}{x}\right)^{0.9}\left(\frac{\rho_G}{\rho_L}\right)^{0.5}\left(\frac{\mu_L}{\mu_G}\right)^{0.1} \qquad [8.1.10]$$

To implement the method for stratified-wavy flow, first the void fraction ε is calculated using the Zivi void fraction given by [8.1.3]. Assuming all the liquid is stratified in the bottom of the tube (neglecting condensate formed on the walls), the angle from the top of the tube to the stratified liquid layer in the bottom θ_{strat} is then determined

$$1-\frac{\theta_{strat}}{\pi} \cong \frac{\arccos(2\varepsilon-1)}{\pi} \qquad [8.1.11]$$

The stratified-wavy heat transfer coefficient is obtained by a proration between the film condensation coefficient on the top perimeter of the tube (left term) and the forced convective heat transfer coefficient on the stratified perimeter (right term) as

$$Nu(x) = \frac{0.23\,Re_{Go}^{0.12}}{1+1.11X_{tt}^{0.58}}\left[\frac{Ga_L\ Pr_L}{Ja_L}\right]^{0.25} + (1-\theta_{strat}/\pi)Nu_{strat} \qquad [8.1.12]$$

Forced convection condensation in the stratified liquid is correlated as

$$Nu_{strat} = 0.0195\,Re_{Ls}^{0.8}\,Pr_L^{0.4}\left(1.376+\frac{c_1}{X_{tt}^{c_2}}\right)^{1/2} \qquad [8.1.13]$$

The value of 1.376 makes this expression match the Dittus-Boelter correlation when x = 0. The liquid Galileo number Ga_L for the tube is

$$Ga_L = \frac{g\rho_L(\rho_L-\rho_G)d_i^3}{\mu_L^2} \qquad [8.1.14]$$

while the vapor only Reynolds number Re_{Go} is

$$Re_{Go} = \frac{\dot{m}d_i}{\mu_G} \qquad [8.1.15]$$

The liquid Jakob number Ja_L defined by [7.5.12],

$$Ja_L = \frac{c_{pL}(T_{sat}-T_w)}{h_{LG}} \qquad [8.1.16]$$

and the liquid Froude number Fr_L is

$$Fr_L = \frac{\dot{m}^2}{\rho_L^2\,g\,d_i} \qquad [8.1.17]$$

The empirical constants c_1 and c_2 are obtained as a function of Fr_L as follows:

For $0 < Fr_L \le 0.7$:

$$c_1 = 4.172 + 5.48\,Fr_L - 1.564\,Fr_L^2 \qquad [8.1.18a]$$

$$c_2 = 1.773 - 0.169\,Fr_L \qquad [8.1.18b]$$

For $Fr_L > 0.7$:

$$c_1 = 7.242 \qquad [8.1.19a]$$

$$c_2 = 1.655 \qquad [8.1.19b]$$

The Soliman (1982) transition criterion for predicting the transition from annular flow to stratified-wavy flow was used to distinguish which heat transfer regime to apply. His method is based on a Froude transition number Fr_{so} given as

$$Fr_{so} = 0.025\, Re_{Ls}^{1.59} \left(\frac{1 + 1.09\, X_{tt}^{0.039}}{X_{tt}} \right)^{1.5} \frac{1}{Ga_L^{0.5}} \qquad [8.1.20]$$

for $Re_{Ls} \le 1250$ and for $Re_{Ls} > 1250$ it is

$$Fr_{so} = 1.26\, Re_{Ls}^{1.04} \left(\frac{1 + 1.09\, X_{tt}^{0.039}}{X_{tt}} \right)^{1.5} \frac{1}{Ga_L^{0.5}} \qquad [8.1.21]$$

While Soliman set the transition from annular flow to wavy flow at $Fr_{so} = 7$, Dobson and Chato noted that a transition value of 20 fit their heat transfer data better and this is the value they used. Their method is implemented as follows:

- For mass velocities greater than 500 kg/m^{2}s (367,896 lb/h ft^2), the annular flow correlation is always utilized;
- For mass velocities less than 500 kg/m^{2}s (367,896 lb/h ft^2), the annular flow correlation is used when $Fr_{so} > 20$;
- For mass velocities less than 500 kg/m^{2}s (367,896 lb/h ft^2) and for $Fr_{so} < 20$, the stratified-wavy correlation is used.

This method does not have a smooth transition in the heat transfer coefficient from annular flow to stratified-wavy flow; instead, it gives a significant step change in value that is not observed experimentally. Other than this inconvenience, their method appears to be the most accurate design method currently available according to Cavallini et al. (1995), who compared it to independent test data. The discontinuity in the heat transfer coefficient may be resolved for now by implementing a simple linear proration based on Fr_{so} between the corresponding calculated heat transfer coefficients at say $Fr_{so} = 7$ with the stratified-wavy correlation and at $Fr_{so} = 20$ with the annular flow correlation.

Tang (1997) has also proposed a simple correlation that is an extension of the Shah (1979) approach and covers reduced pressures from 0.2 to 0.53 and mass velocities from 300 to 810 kg/m^{2}s. His correlation is applicable to annular flow only and is:

$$\frac{\alpha(x)\, d_i}{k_L} = 0.023\, Re_L^{0.8}\, Pr_L^{0.4} \left[1 + 4.863 \left(\frac{-x \ln p_r}{1 - x} \right)^{0.836} \right] \qquad [8.1.22]$$

Recent test data for intube condensation for an 8 mm (0.315 in.) tube for a wide range of pressures (0.246 to 3.15 MPa, 35.7 to 456.8 psia) have been reported by Cavallini et al. (2001) for five fluids: R-134a, R-125, R-32, R-410A and R-236ea. They covered mass velocities from 100 to 750 kg/m^{2}s (73,579 to 551,844 lb/h ft^2) and vapor qualities from 0.15 to 0.85 in quasi-local type of tests.

El Hajal, Thome and Cavallini (2003) proposed a phenomenological condensation model based on local flow patterns and interfacial wave effects for condensation inside plain tubes for a very wide range of

parameters: mass velocities from 16 to 1532 kg/m^{2}s (11773 to 1127230 lb/h ft^2), tube internal diameters from 3.14 to 21.4 mm (0.124 to 0.843 in.), reduced pressures from 0.02 to 0.8, and vapor qualities from 0.03 to 0.97. They used the El Hajal, Thome and Cavallini (2003) flow pattern map for condensation, described in Chapter 12, to predict the local flow patterns in their heat transfer model. So far for heat transfer and flow patterns, the method has been compared with the following twenty fluids: ammonia, R-11, R-12, R-22, R-32, R-113, R-123, R-125, R-134a, R-236ea, R-32/R-125 near azeotrope, R-402A, R-404A, R-407C, R-410A, R-502, propane, n-butane, iso-butane and propylene. They showed not only that the heat transfer model was accurate statistically…85% of the eleven original refrigerants in their database from nine different labs, representing a total of 1850 data points, were predicted within ±20% but also that it followed the trends within the database well with respect to vapor quality, tube diameter, mass velocity, reduced pressure, void fraction, etc. Below is a detailed description of the model.

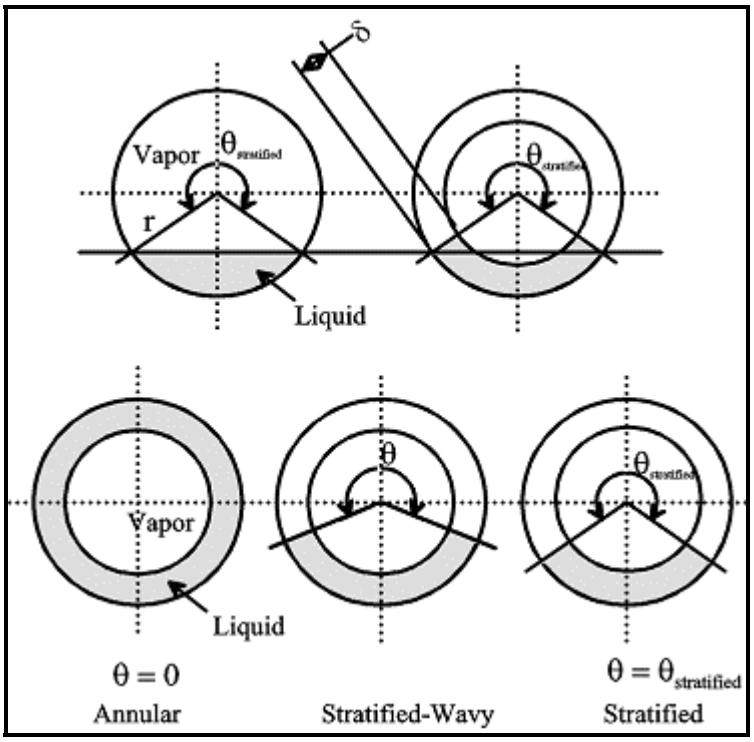

Figure 8.4. Simplified two-phase flow structures assumed for annular, stratified-wavy and stratified flow regimes.

Simplified flow structures for condensation in horizontal tubes. The same simplified flow structures assumed for evaporation inside horizontal tubes by Kattan, Thome and Favrat (1998c) were applied to condensation, differing only in that the upper perimeter of the tube in a stratified type of condensing flow is wetted by film condensation rather than dry during evaporation. The Thome-El Hajal-Cavallini condensation model assumes three simplified geometries for describing annular flow, stratified-wavy flow and fully stratified-wavy flow as shown in Figure 8.4. For annular flow (bottom left), a uniform liquid film thickness of δ is assumed and the effects due to gravity ignored. For fully stratified flow, the stratified geometry (upper left) is converted to an equivalent geometry (upper right) with the same angle of stratification and cross-sectional area occupied by the liquid, but with the liquid distributed as a truncated annular ring of uniform thickness δ. In stratified-wavy flow (lower middle diagram), the interfacial waves are small and do not reach the top of the tube and hence the upper perimeter would remain dry if not for the condensate that forms, again assuming that the stratified liquid creates an annular truncated ring. Thus, the angle θ varies between its maximum value of θ_{strat} at the threshold to fully

stratified flow and its minimum value of zero at the threshold to annular flow. Importantly, these three simple geometries yield a smooth geometrical transition from one flow structure to another.

Heat transfer model. Referring to Figure 8.5, the heat transfer model for stratified types of flow have convective heat transfer applied to the stratified perimeter subtended by $(2\pi - \theta)$ while film condensation is applied to the upper perimeter subtended by θ with the condensate flowing downwards into the stratified liquid below. For annular flow, convective condensation heat transfer occurs around the entire perimeter without any film condensation. It was further found that the annular flow model worked well for intermittent flow regimes and for the limited amount of mist flow data available. Hence, the annular flow heat transfer model is applied to both, maintaining the simplicity of the model, but no bubbly flow heat transfer data were found in the literature and hence no bubbly flow heat transfer model was proposed (which does not fall within common design conditions anyway).

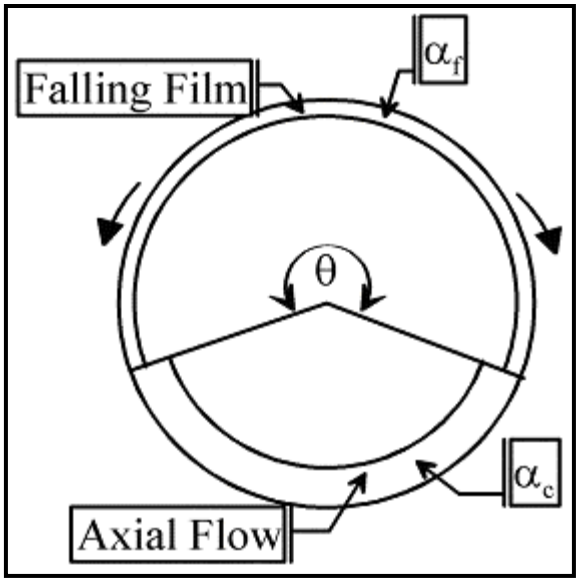

Figure 8.5. Condensation heat transfer model showing the axial convective heat transfer and the falling film heat transfer perimeters around the tube.

Both of these mechanisms have been included in some previous models, such as that of Dobson and Chato (1998) while applying the Nusselt (1916) film condensation model to the upper perimeter of a horizontal tube with stratified flow was first proposed by Chato (1962). In the Thome-El Hajal-Cavallini model, the above two heat transfer mechanisms are applied to their respective heat transfer surface areas as shown in Figure 8.5. The convective condensation heat transfer coefficient α_c is applied to the perimeter wetted by the axial flow of liquid film, which refers to the entire perimeter in annular, intermittent and mist flows but only the lower part of the perimeter in stratified-wavy and fully stratified flows. The axial film flow is assumed to be turbulent. The film condensation heat transfer coefficient α_f is applied to the upper perimeter that would otherwise be dry for stratified-wavy and fully stratified flows. The Nusselt (1916) falling film theory is used to obtain α_f, which assumes the falling film is laminar (which is essentially always the case for the tube diameters in question here). The effect of vapor shear on this falling film is ignored. Heat transfer coefficients for stratified types of flow are known experimentally to be a function of the wall temperature difference while those for annular flow are not. This effect is thus included here through the Nusselt falling film equation.

The general expression for the local perimeter-averaged condensing heat transfer coefficient $\alpha(x)$ is thus:

$$\alpha(x) = \frac{\alpha_f \theta + (2\pi - \theta)\alpha_c}{2\pi} \qquad [8.1.23]$$

In this expression, θ is the falling film angle around the top perimeter. Hence, $\alpha(x)$ is equal to α_c for annular, intermittent and mist flows with $\theta = 0$. The stratified angle θ_{strat} is calculated from the following implicit geometric equation:

$$A_L = \frac{d_i^2}{8}\left[(2\pi - \theta_{strat}) - \sin(2\pi - \theta_{strat})\right] \quad [8.1.24]$$

The cross-sectional area occupied by the liquid phase A_L is

$$A_L = (1-\varepsilon)A \quad [8.1.25]$$

and the cross-sectional area occupied by the vapor A_G is

$$A_G = \varepsilon A = 1 - A_L \quad [8.1.26]$$

The total cross-sectional area of the tube is A and ε is the local cross-sectional void fraction, which is determined using the logarithmic mean void fraction using the Steiner (1993) version of the Rouhani drift flux model, see Chapter 17, and the homogeneous model in order to cover the range from low to high reduced pressures. The logarithmic mean void fraction ε was defined as:

$$\varepsilon = \frac{\varepsilon_H - \varepsilon_r}{\ln(\varepsilon_H/\varepsilon_r)} \quad [8.1.27]$$

The homogeneous void fraction ε_H is:

$$\varepsilon_H = \frac{1}{1+\left(\frac{1-x}{x}\right)\frac{\rho_G}{\rho_L}} \quad [8.1.28]$$

Steiner (1993) gives the horizontal tube version of the Rouhani void fraction ε_{ra} as:

$$\varepsilon_r = \frac{x}{\rho_G}\left(\left[1+0.12(1-x)\right]\left[\frac{x}{\rho_G}+\frac{1-x}{\rho_L}\right]+\frac{1.18\ (1-x)\left[g\sigma(\rho_L-\rho_G)\right]^{0.25}}{\dot{m}\rho_L^{0.5}}\right)^{-1} \quad [8.1.29]$$

For annular, intermittent and mist flows, θ = 0. For fully stratified flows, $\theta = \theta_{strat}$. For stratified-wavy flow, the stratified angle θ is obtained by assuming a quadratic interpolation between the maximum value of θ_{strat} at the transition from stratified-wavy to fully stratified flow and 0 at the transition from stratified-wavy to annular or intermittent flow, such that:

$$\theta = \theta_{strat}\left[\frac{(\dot{m}_{wavy} - \dot{m})}{(\dot{m}_{wavy} - \dot{m}_{strat})}\right]^{0.5} \quad [8.1.30]$$

The transition values at the vapor quality in question are determined from their respective transition equations in the condensation flow pattern map of El Hajal, Thome and Cavallini (2003) in Chapter 12. To avoid the iterative calculation in [8.1.24] to solve for θ_{strat}, a nearly equivalent explicit expression of Biberg (1999) is evaluated using the value of ε from [8.1.27]:

$$\theta_{strat} = 2\pi - 2\left\{\begin{array}{l}\pi(1-\varepsilon)+\left(\frac{3\pi}{2}\right)^{1/3}\left[1-2(1-\varepsilon)+(1-\varepsilon)^{1/3}-\varepsilon^{1/3}\right] \\ -\frac{1}{200}(1-\varepsilon)\varepsilon\left[1-2(1-\varepsilon)\right]\left[1+4\left((1-\varepsilon)^2+\varepsilon^2\right)\right]\end{array}\right\} \quad [8.1.31]$$

The convective condensation heat transfer coefficient α_c in the annular liquid film is obtained from the following turbulent liquid film correlation:

$$\alpha_c = c\,Re_L^n\,Pr_L^m\,\frac{k_L}{\delta}f_i \quad [8.1.32]$$

where the liquid film Reynolds number Re_L is based on the mean liquid velocity of the liquid flow through A_L as:

$$Re_L = \frac{4\dot{m}(1-x)\delta}{(1-\varepsilon)\mu_L} \quad [8.1.33]$$

and the liquid Prandtl number Pr_L is defined as:

$$Pr_L = \frac{c_{pL}\mu_L}{k_L} \quad [8.1.34]$$

The values of the empirical constants c, n and m were determined from the heat transfer database whereas δ is the thickness of the liquid film. The best value of m was determined to be m = 0.5, i.e. the same value found by Labuntsov (1957) for turbulent falling film condensation on a vertical plate, which is larger than the value of 0.4 in the Dittus and Boelter (1930) single-phase tubular flow correlation. The best values of c and n were found statistically to be c = 0.003 and n = 0.74 from the annular flow condensation database.

In the above expressions, the liquid film thickness δ is obtained by solving the following geometrical expression:

$$A_L = \frac{(2\pi-\theta)}{8}\left[d_i^2-\left(d_i^2-2\delta\right)^2\right] \quad [8.1.35]$$

where d_i is the internal diameter of the tube. If the liquid occupies more than one-half of the cross-section of the tube in a stratified-wavy or fully stratified flow at low vapor quality, i.e. when $\varepsilon < 0.5$, this expression yields $\delta > d_i/2$, which is not geometrically realistic. Hence, whenever $\delta > d_i/2$ then δ is set equal to $d_i/2$ in their method.

Interfacial surface roughness of the liquid film flow was identified as a new influential parameter on heat transfer in their intube condensation model for the following reasons: (i) the shear of the high speed vapor core is transmitted to the liquid film across the interface and hence increases the magnitude and number of the waves generated at the interface, which in turn increases the available surface area for condensation, tending to increase heat transfer and (ii) the interfacial waves are non-sinusoidal and tend to reduce the mean thickness of the film, again increasing heat transfer. These two aspects are analogous to

the enhancement correction factor of Kutateladze (1963) for interfacial ripples on Nusselt film condensation on a vertical plate. Interfacial roughness and wave formation are also directly relatable to entrainment of liquid droplets into the vapor core, which reduces the thickness of the liquid film and increases heat transfer. Furthermore, interfacial shear tends to create vortices within the liquid film, which also increase heat transfer.

The interfacial roughness is proportional to the interfacial shear τ_i, whereas τ_i depends on the velocity difference between the two phases, $(u_G - u_L)$, and u_G and u_L are the mean velocities of the vapor and liquid phases in their respective cross-sectional areas A_G and A_L determined with the void fraction:

$$u_L = \frac{\dot{m}(1-x)}{\rho_L(1-\varepsilon)} \qquad [8.1.36]$$

$$u_G = \frac{\dot{m}x}{\rho_G \varepsilon} \qquad [8.1.37]$$

Usually $u_G >> u_L$, so then $(u_G - u_L) \approx u_G$. Normalizing the vapor velocity with that of the liquid gives the slip ratio, u_G/u_L, typical of void fraction models, and the interfacial shear is thus proportional to (u_G/u_L). Consequently, the interfacial roughness $\Delta\delta$ was assumed to be proportional to $(u_G/u_L)^p$ where the exponent p was to be determined. The wavelength of the interfacial waves should be related to the one-dimensional Taylor instability wavelength λ_T for an unsupported liquid film on the top of the tube, the latter which is calculated as:

$$\lambda_T\left[\frac{(\rho_L - \rho_G)g}{\sigma}\right]^{1/2} = 2\pi\sqrt{3} \qquad [8.1.38]$$

Assuming that the interfacial waves have characteristic wavelengths that can be scaled relative to the film thickness, then substituting δ for λ_T means that the interfacial roughness $\Delta\delta$ is described by follow relationship:

$$\Delta\delta \propto \left[\frac{(\rho_L - \rho_G)g\delta^2}{\sigma}\right]^r \qquad [8.1.39]$$

where the term inside the brackets is non-dimensional and r is an unknown exponent. The interfacial roughness correction factor f_i in [8.1.32] acts on α_c to include the effects of vapor shear and interfacial instability on wave formation. Adjusting the values of p and r based on the test data to nominal values of ½ and ¼ but without introducing any additional empirical constants, f_i is determined for all flow regimes except fully stratified flow as:

$$f_i = 1 + \left(\frac{u_G}{u_L}\right)^{1/2}\left(\frac{(\rho_L - \rho_G)g\delta^2}{\sigma}\right)^{1/4} \qquad [8.1.40]$$

The interfacial roughness correction factor f_i tends to unity as the film becomes very thin (physically, the roughness must be proportional to film thickness) whereas f_i increases with the slip ratio u_G/u_L (again physically reasonable). Furthermore, f_i tends to decrease as σ increases since surface tension acts to

smooth out the waves. For fully stratified flow, interfacial waves are progressively damped out and hence the above expression becomes

$$f_i = 1 + \left(\frac{u_G}{u_L}\right)^{1/2}\left(\frac{(\rho_L - \rho_G) g \delta^2}{\sigma}\right)^{1/4}\left(\frac{\dot{m}}{\dot{m}_{strat}}\right) \quad \text{for} \quad \dot{m} < \dot{m}_{strat} \qquad [8.1.41]$$

This approach produces a smooth variation in $\alpha(x)$ across the stratified flow transition boundary just like for all the other transition boundaries.

The film condensation heat transfer coefficient α_f is obtained from the Nusselt (1916) condensation theory for laminar flow of a falling film, see Chapter 7, applied here to the internal perimeter of the tube. Rather than integrating his method from the top of the tube to the stratified liquid layer to obtain α_f, which would be more theoretically satisfying, it was found sufficient to use the mean value for condensation around the perimeter from top to bottom with its analytical value of 0.728. Hence, α_f is:

$$\alpha_f = 0.728\left[\frac{\rho_L(\rho_L - \rho_G) g\, h_{LG}\, k_L^3}{\mu_L d_i (T_{sat} - T_w)}\right]^{\frac{1}{4}} \qquad [8.1.42]$$

Alternatively, the heat flux version of the above equation is given by:

$$\alpha_f = 0.655\left[\frac{\rho_L(\rho_L - \rho_G) g\, h_{LG}\, k_L^3}{\mu_L d_i\, q}\right]^{\frac{1}{3}} \qquad [8.1.43]$$

where the leading constant 0.655 comes from $0.728^{4/3}$.

The above heat transfer method cannot be evaluated at $\varepsilon = 1.0$ because of division by zero. Thus, when $x > 0.99$, x is reset to 0.99. Also, the lower limit of applicability is $x \geq 0.01$ while the range of the test data was for $0.97 > x > 0.03$.

Implementation. The Thome-El Hajal-Cavallini flow pattern based intube condensation heat transfer model is implemented as follows:

1. Determine the local vapor void fraction using [8.1.27];
2. Determine the local flow pattern using the flow pattern map and any necessary transition velocities at the same value of x;
3. Identify the type of flow pattern (annular, intermittent, mist, stratified-wavy or stratified);
4. If the flow is annular or intermittent or mist, then $\theta = 0$ and α_c is determined with [8.1.32] and $\alpha(x) = \alpha_c$ in [8.1.23] where δ is obtained by solving [8.1.35] and f_i with [8.1.40].
5. If the flow is stratified-wavy, θ_{strat} and θ are calculated using [8.1.31] and [8.1.30], then α_c and α_f are calculated using [8.1.32] and [8.1.42] or [8.1.43], and finally $\alpha(x)$ is determined using [8.1.23] where δ is obtained with [8.1.35] and f_i with [8.1.40].
6. If the flow is fully stratified, θ_{strat} is obtained from [8.1.31] and θ_{strat} is set equal to θ, then α_c and α_f are calculated using [8.1.32] and [8.1.42] or [8.1.43], and $\alpha(x)$ is determined using [8.1.23] where δ is obtained with [8.1.35] and f_i is determined with [8.1.41].

Comparison to Refrigerant Database. The new model was primarily developed using the heat transfer database of Cavallini et al. (1999, 2001) and then the other eight independent studies were used to determine its general applicability. Figure 8.6 shows the new model compared to the Cavallini data and Figure 8.7 depicts a comparison to all 1850 data, except the experimental hydrocarbon data which had unrealistic trends at low mass velocities, where about 85% are predicted within ±20%.

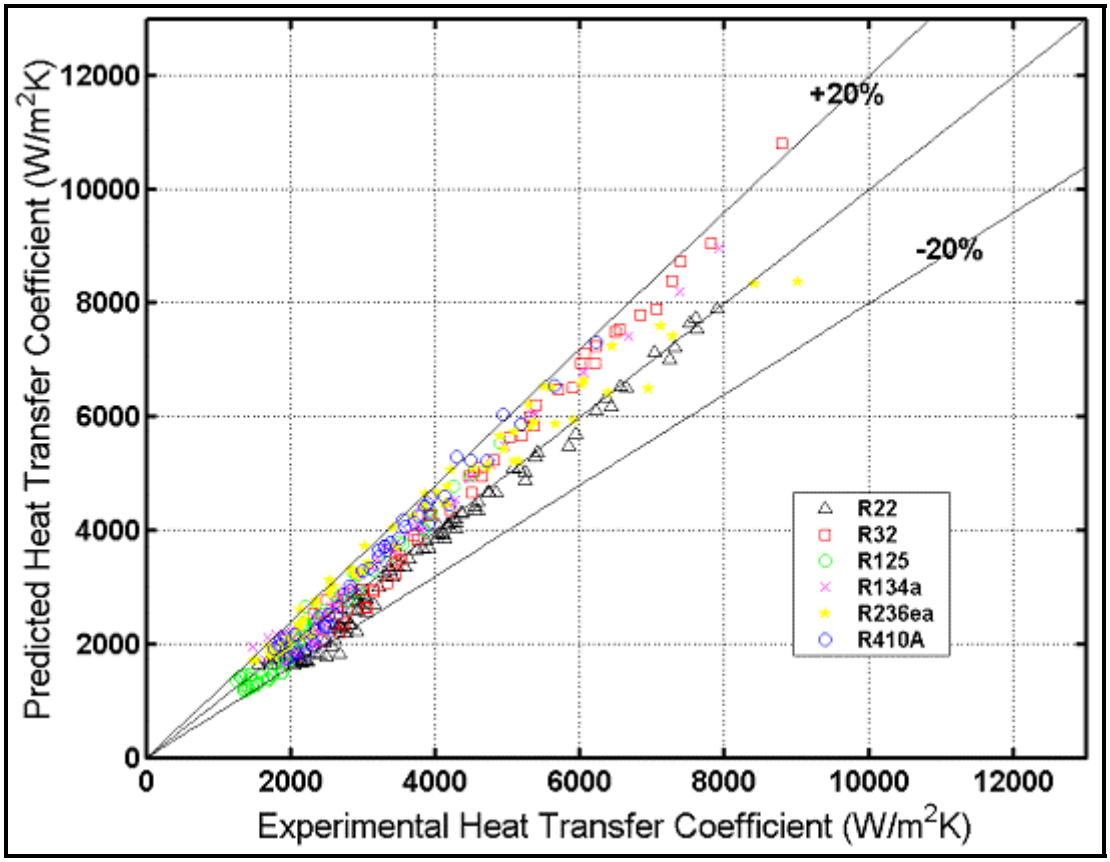

Figure 8.6. Comparison of the Thome-El Hajal-Cavallini model to the data of Cavallini et al.(1999, 2001) for six refrigerants in an 8.0 mm (0.315 in.) tube.

Simulations for R-410A. The heat transfer model and flow pattern map have been simulated for R-410A condensing at 40°C (104°F) in an 8 mm (0.315 in.) diameter tube. The flow pattern map for three different refrigerants, including R-410A, at these conditions is shown in Figure 8.8. The heat transfer coefficients at q = 40 kW/m^2 (12682 Btu/h ft^2) are shown in Figure 8.9 for a range of mass velocities. At 30 kg/m^{2}s (22074 lb/h ft^2), the flow is in the stratified (S) regime from inlet to outlet and the heat transfer coefficient falls off slowly with decreasing vapor quality. At 200 kg/m^{2}s (147163 lb/h ft^2), the flow enters in the annular (A) regime and then passes through the intermittent (I) and stratified-wavy (SW) regimes. At 500 kg/m^{2}s (367906 lb/h ft^2), the flow enters in the annular (A) regime, converts to intermittent (I) flow and leaves in this same regime. The sharp decline in $\alpha(x)$ with decreasing x at high vapor qualities comes from the rapid growth of the annular film thickness δ. At 800 kg/m^{2}s (588650 lb/h ft^2), the flow enters in the mist flow (MF) regime, goes into the annular (A) regime and leaves in the intermittent (I) regime.

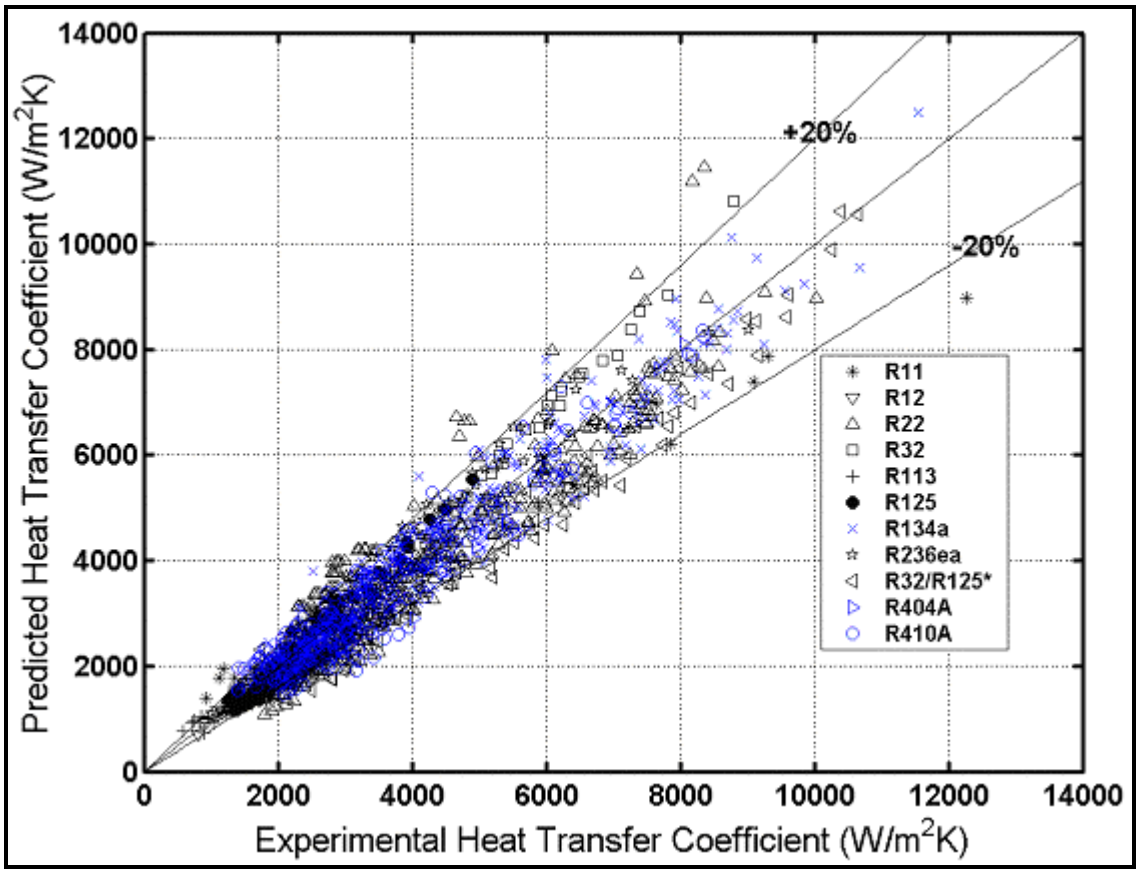

Figure 8.7. Comparison of the Thome-El Hajal-Cavallini model to all their databases for eleven refrigerants.

Figure 8.8. Flow pattern transitions for R-134a, R-22 and R-410A in an 8 mm tube at Tsat = 40°C, using for simplicity a fixed value of mass velocity of 300 kg/m2s to evaluate void fractions in preparation of the diagram (in application of the model, the actual mass actual mass velocity is always used for all calculations).

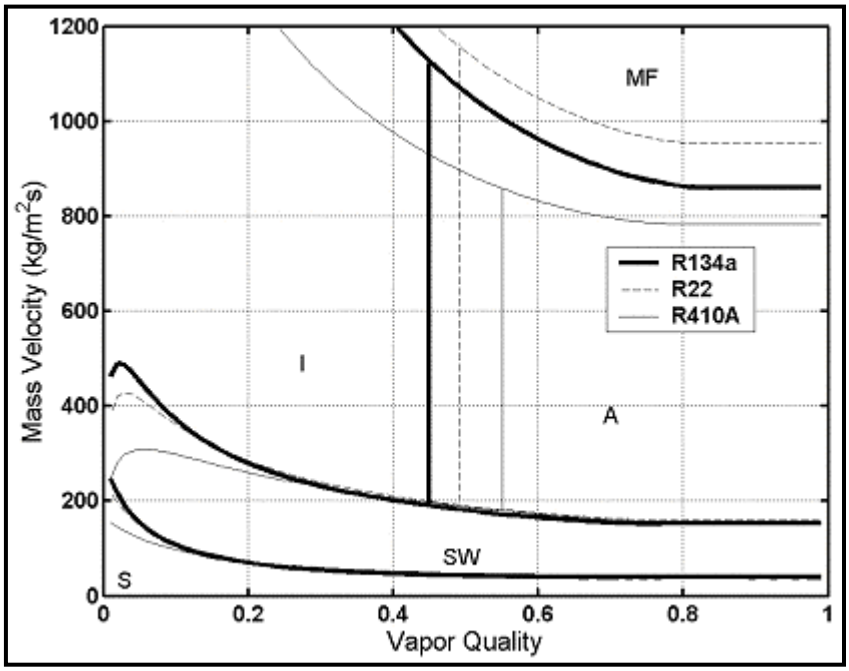

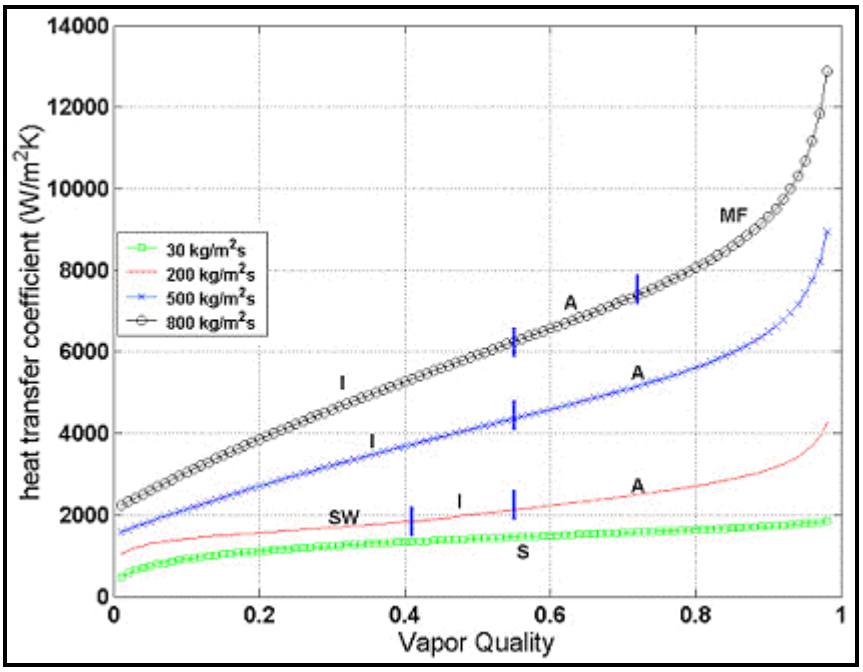

Figure 8.9. Simulation of heat transfer for R-410A at Tsat = 40°C in an 8 mm tube at a heat flux of 40 kW/m2 for 4 mass velocities.

As can be seen, the new heat transfer model predicts the variation in the local heat transfer coefficients across flow pattern transition boundaries without any discontinuity in the value of $\alpha(x)$. This, for example was a problem in the Dobson and Chato (1998) method and also in the recent Cavallini et al. (2002) method going through the transition into their slug flow regime.

Figure 8.10 depicts a similar simulation at heat fluxes of 10 and 40 kW/m^2 at 200 kg/m^{2}s (3170 and 12682 Btu/h ft^2 at 147163 lb/h ft^2), where the lower heat flux is more representative of typical design conditions. Here, the flow enters in the annular regime and coverts to intermittent flow and then finally becomes stratified-wavy at about x = 0.41. In the stratified-wavy regime, the film condensation heat transfer mechanism kicks in around the upper perimeter of the tube and the effect of heat flux is quite evident, where the lower heat flux creates a thinner condensate film and hence a larger heat transfer coefficient.

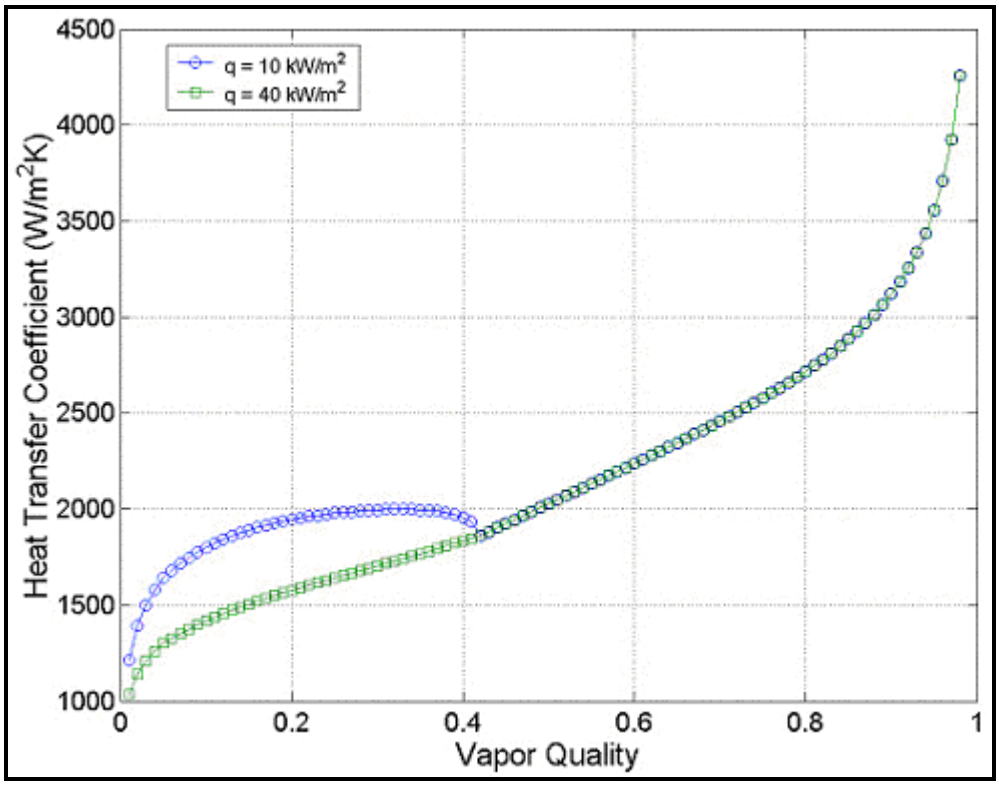

Figure 8.10. Simulation of heat transfer for R-410A at Tsat = 40°C in an 8 mm tube at heat fluxes of 10 and 40 kW/m2 for a mass velocity of 200 kg/m2s.

8.2 Condensation in Horizontal Microfin Tubes

Shizuya, Itoh and Hijikata (1995) have done an extensive comparative study between a microfin tube and a plain tube for R-22, R-142b, R-114 and R-123. Their microfin tube had 55 fins with a 14° helix angle of 0.19 mm height and an internal area ratio 1.6 times that of an equivalent plain tube. The microfin tube had an internal diameter of 6.26 mm while that of the plain tube was 6.16 mm. Figure 8.11 depicts their comparison, where the flow patterns observed during the tests were also noted. The level of augmentation tends to be larger for wavy-slug flow than for annular flow.

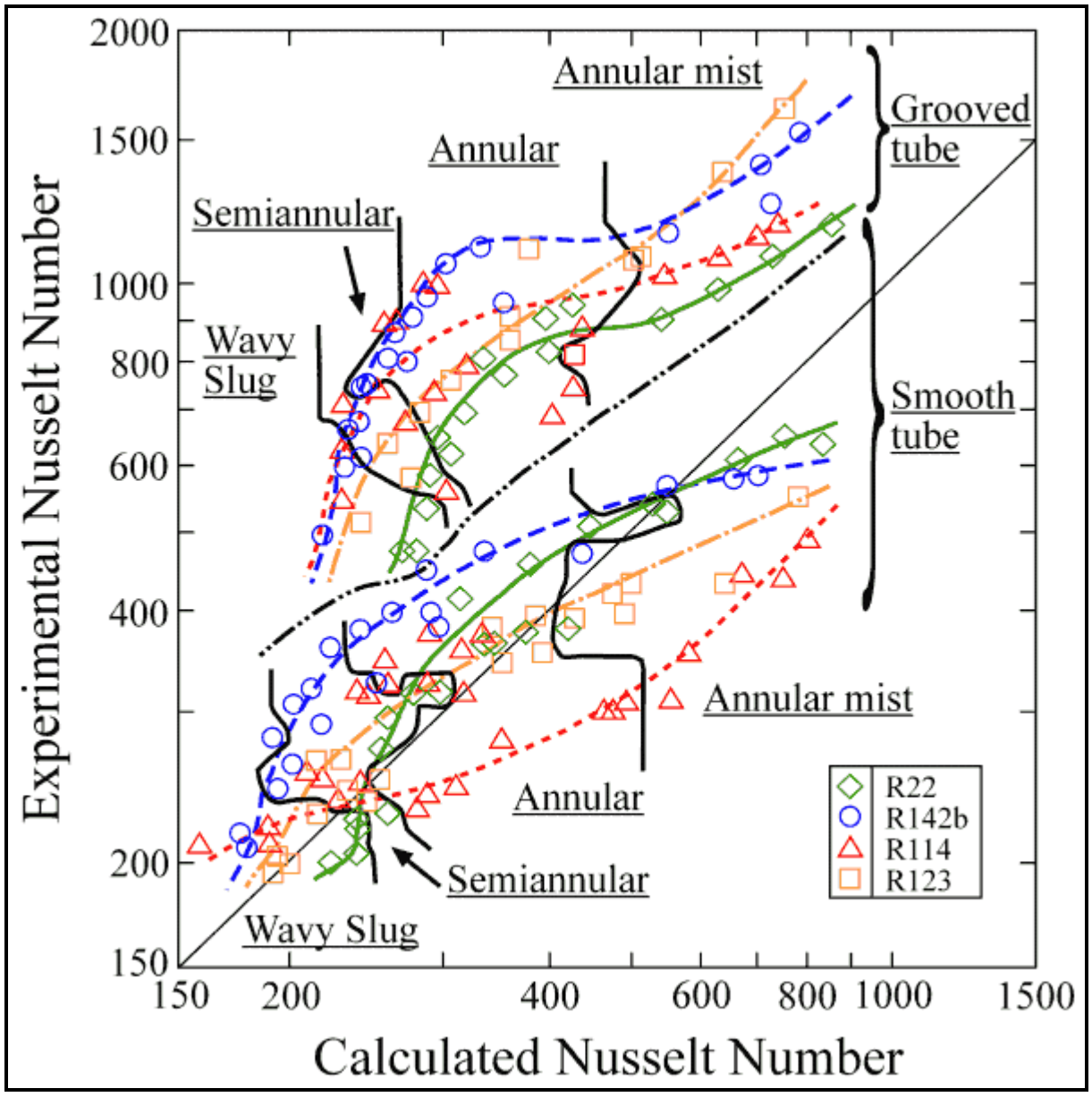

Figure 8.11. Comparison of microfin tube to plain tube performance by Shizuya, Itoh and Hijikata (1995) for four refrigerants.

Muzzio, Niro and Arosio (1998) have measured intube-condensing coefficients for a plain tube, a microfin tube with alternating fin heights (VA), a conventional microfin tube (V) and microfin tube with a screw profile (W). Their results for R-22 are shown in Figure 8.12. As is typical of microfin condensation tests, the level of heat transfer augmentation is highest at low mass velocities and tends to fall off towards the value of the area ratio at high mass velocities.

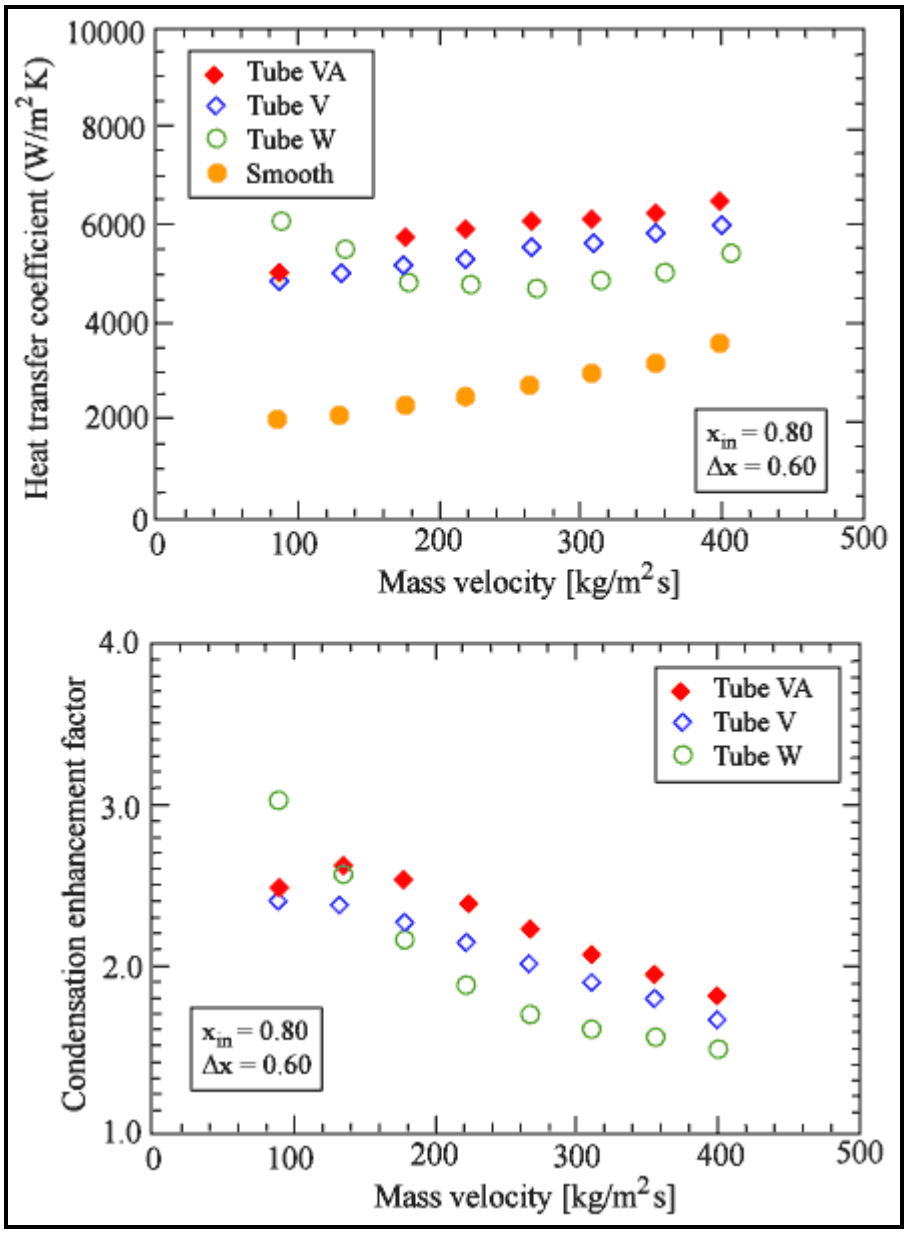

Figure 8.12. Condensation heat transfer and enhancement factor versus mass velocity at an inlet vapor quality of 0.8 and a vapor quality change of 0.6 obtained by Muzzio, Niro and Arosio (1998).

Numerous other tests have been done on condensation inside microfin tubes. Some of the following are the more important studies since 1990:

- Koyama, Miyara, Takamatsu and Fujii (1990) measured condensing coefficients for R-22 and R-114.
- Eckels and Pate (1991a) presented a detailed comparison of mean coefficients for R-134a versus R-12.
- Chiang (1993) ran tests with R-22 inside helical and axial microfin tubes, including tests on tubes that had already been mechanically expanded.
- Torikoshi and Ebitsu (1994) ran tests on R-22 and refrigerant mixtures in a microfin tube.

- Du, Xin and Huang (1995) measured condensing coefficients for R-11 in two 2-dimensional axial microfin tubes and three 3-dimensional axial microfin tubes whose fins were cross-cut. In annular flow the cross-cutting provided 34-144% improvement while in stratified flow the improvement was 31-97%.
- Chamra and Webb (1995) also ran comparative tests on 2-d and 3-d microfin geometries for R-22, but found only a marginal improvement of 5-15% from the cross-cutting.
- Uchida, Itoh, Shikazono and Kudoh (1996) also ran similar comparative tests of 2-d and 3-d microfin tube geometries for R-22.
- Dunn (1996) carried out an excellent experimental program on a 9.53 mm (3/8 in.) Wolverine Tube microfin tube Turbo-A for R-22 and R-134a and three azeotropic mixtures. He observed that R-134a had equal or better performance than R-22 while R-410A performed similar to R-22.
- Kedzierski and Goncalves (1997) reported microfin condensation data for R-134a, R-125, R-32 and R-410A. Using a temperature profile approach, they reported true local condensing data rather than quasi-local data typical of other studies.

Methods currently available for simulating local heat transfer coefficients during condensation in microfin tubes are described in Cavallini et al. (1999).

8.3 Condensation of Condensable Mixtures in Horizontal Tubes

The Silver-Bell-Ghaly method [Silver (1947) and Bell and Ghaly (1973)] is successfully used to predict condensation of miscible mixtures where all components are condensable but no non-condensable gases are present. When condensing a mixture, the vapor phase must be cooled as the dew point temperature of the mixture falls along the tube, in addition to removing the latent heat. Hence, the process is controlled by condensation and by single-phase cooling of the vapor. This approach assumes two things with respect to cooling of the vapor:

- Mass transfer has no effect on the single-phase heat transfer process in the vapor.
- The vapor occupies the entire tube cross section in determining the vapor phase heat transfer coefficient.

The error in ignoring the first assumption becomes significant for mixtures with large condensing temperature ranges, so their method is reliable for mixtures with small to medium condensing ranges (say smaller than 30 K). The second assumption is conservative since interfacial waves in annular flows augment the vapor phase heat transfer coefficient. The effective condensing heat transfer coefficient α_{eff} for condensation of a mixture is calculated by the method as

$$\frac{1}{\alpha_{eff}} = \frac{1}{\alpha(x)} + \frac{Z_G}{\alpha_G} \qquad [8.3.1]$$

To implement this expression, the condensation heat transfer coefficient $\alpha(x)$ is obtained with an intube correlation for pure fluids in the previous section but inputting the local physical properties of the mixture. The single-phase heat transfer coefficient of the vapor α_G is calculated with the Dittus-Boelter turbulent flow correlation using the vapor fraction of the flow in calculating the vapor Reynolds number. The parameter Z_G is the ratio of the sensible cooling of the vapor to the total cooling rate:

$$Z_G = x\, c_{pG} \frac{dT_{dew}}{dh} \qquad [8.3.2]$$

where x is the local vapor quality, c_{pG} is the specific heat of the vapor and dT_{dew}/dh is the slope of the dew point temperature curve with respect to the enthalpy of the mixture as it condenses, i.e. the slope of the condensation curve. This method has been applied to hydrocarbon mixtures and more recently to binary and ternary zeotropic refrigerant blends by Cavallini et al. (1995) and to binary refrigerant mixtures by Smit, Thome and Meyer (2001). For a more complete description of multi-component condensation, refer to Butterworth (1983).

Table 8.1. Condensation heat transfer database for zeotropic mixtures considered by Del Col, Cavallini and Thome (2005).

Study	*Data Pts.*	*Mixture (liquid mass fraction)*	*d_i [mm]*	*T_{sat} [°C]*	*ΔT_{qlide} [°C] **	*(T_{sat}-T_w) [°C]*	*Mass Velocity [kg/m^{2}s]*
Cavallini et al. (1999)	38	R-407C	8.0	38-49	4.9	4.5-13	104-755
Cavallini et al. (2000)	43	R-125/R-236ea (46/54%)	8.0	39-57	21.2	6.5-18	102-753
	31	R-125/R-236ea (63/37%)	8.0	36-55	16.9	5.5-13.5	96-751
	24	R-125/R-236ea (28/72%)	8.0	35-56	21.9	5.7-13.9	98-743
Lee (1994)	27	R-22/R-124 (20/80%)	7.5	19-44	5.5	9.4-19.3	215-305
	26	R-22/R-124 (50/50%)	7.5	22-39	6.7	10.9-19.2	167-369
	24	R-22/R-124 (80/20%)	7.5	22-37	3.6	7.7-15.8	174-358
Kim et al. (1996)	213	R-290/R-600 (25/75%)	8.0	45-54	10.5	2.8-6.9	65-154
	205	R-290/R-600 (50/50%)	8.0	44-55	12.2	3.5-6.9	57-172
	241	R-290/R-600 (75/25%)	8.0	46-54	8.2	3.5-7.3	89-191

(*) Values of ΔTglide are mean values of the range tested in each study.

Del Col, Cavallini and Thome (2005) recently made a detailed study on condensation of mixtures inside plain horizontal tubes covering a multi-laboratory database, shown in Table 8.1. The model by Thome, El Hajal (2003) for local condensation heat transfer coefficient of pure fluids and azeotropic mixtures and the accompanying flow pattern map of El Hajal, Thome and Cavallini (2003) were used as the starting point. It was extended to zeotropic mixtures by modifying the Silver-Bell-Ghaly method already described above. The additional heat transfer resistance created by the mixture was applied to both the convective and the film coefficients, including the effect of interfacial roughness on the vapor heat transfer coefficient α_G acting on the convective film. A non-equilibrium mixture factor was also introduced to account for non-equilibrium effects on stratified and stratified-wavy flow regimes. The new

method requires much less computational effort than theoretical mass diffusion methods, but still provides accurate predictions of the local heat transfer data and is more accurate than the original Silver-Bell-Ghaly method. Compared against the database shown in Table 8.1 obtained from three independent laboratories, which includes ten different mixtures with temperature glides ranging from 3.5 to 22.8°C (6.3 to 41.0°F) for both refrigerant and hydrocarbon mixtures, the method predicted 98% of the refrigerant heat transfer coefficients measured by Cavallini et al. (1999, 2000) to within ±20% and 85% of the halogenated plus hydrocarbon refrigerant heat transfer coefficients measured by independent researchers to within ±20%. This new method is described below.

Heat transfer database. The database of condensation heat transfer coefficients available for their study involved four mixture systems representing 10 different zeotropic mixture compositions with a wide range of temperature glides and test conditions. The database covered HCFCs, HFCs and HCs (hydrocarbons). The temperature glide was defined as the difference between the dew point temperature and the bubble point temperature at a fixed pressure and bulk composition. One set of data of Cavallini and coworkers covered R-407C and three mixtures of R-125/R-236ea. The other blends they tested had higher temperature glides from mixing two HFC fluids having far different saturation temperatures, R-125 and R-236ea. R-125 was the "high pressure" fluid whereas R-236ea was the "low pressure" fluid. The data set by Lee (1994) is for the mixture R-22/R-124 at three different mass compositions while the data set of Kim, Chang and Ro (1996) includes heat transfer data on propane/butane mixtures. Figure 8.13 shows some of the test data considered.

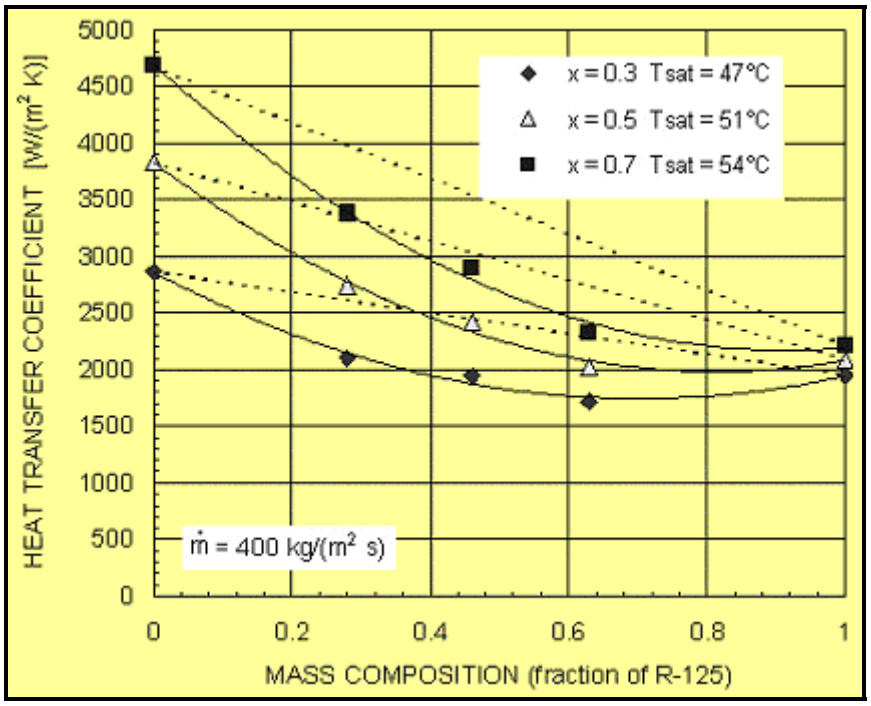

Figure 8.13. Condensation heat transfer coefficients for R-236fa, R-125 and three of their mixtures from Cavallini et al. (2000) at three different mean vapor qualities at the noted saturation temperatures.

The term $1/\alpha(x)$ in [8.3.1] represents the condensate layer resistance and for a mixture it is typically computed using a pure fluid model inputting the liquid mixture properties. The second term in [8.3.1] represents the thermal resistance to cool the vapor flow along the channel to the local, declining saturation

temperature. Primarily, Del Col, Cavallini and Thome (2005) have introduced three improvements to the original Silver-Bell-Ghaly method:

The vapor phase heat transfer coefficient α_G is corrected for the enhancing effect of the interfacial waves (the waves function essentially like internal ribs in a tube and hence increase the vapor phase heat transfer coefficient above the Dittus-Boelter value);

The interfacial waves are a function of flow pattern as only the perimeter of the tube with axial convection has interfacial waves in the underlying pure fluid model while the upper perimeter with falling film condensation does not and hence the angle θ becomes a parameter affecting α_G in stratified types of flows of mixtures;

Non-equilibrium effects are included, that become more significant in stratified types of flows due to the reduction of mixing.

Similar to the procedure for pure fluids described earlier, the perimeter-averaged local heat transfer coefficient for the mixture α_{eff} is obtained from a proration of the film condensation coefficient of the mixture α_{fm} and the convective condensation coefficient of the mixture α_{cm}, by accounting for the different perimeters pertaining to the two mechanisms:

$$\alpha_{eff} = \frac{\alpha_{fm}\theta + (2\pi - \theta)\alpha_{cm}}{2\pi} \qquad [8.3.3]$$

Applying the Thome-El Hajal-Cavallini pure fluid heat transfer model and its flow pattern map to mixtures, the method remains exactly the same as presented earlier in this chapter except for the changes described below. Furthermore, the physical properties of the local mixture composition are used in all calculations. The temperature glide is denoted as ΔT_{glide} and Δh_m refers to the change of enthalpy of the mixture including both the latent heat and the sensible cooling effects on the liquid and vapor phases. θ is the falling film angle around the top perimeter of the tube (Figure 8.4) and is computed using [8.1.30]. The convective condensation heat transfer coefficient is obtained from the Bell and Ghaly approach, as follows:

$$\alpha_{cm} = \left[\frac{1}{\alpha_c} + R_c\right]^{-1} \qquad [8.3.4]$$

α_c is computed from the equations for the pure fluid model. The appropriate Bell and Ghaly resistance R_c can be calculated as follows:

$$R_c = x c_{pG} \frac{\Delta T_{glide}}{\Delta h_m} \frac{1}{\alpha_G f_i} \qquad [8.3.5]$$

The resistance R_c is a function of the vapor phase heat transfer coefficient referred to the vapor-liquid interface. Thome, El Hajal and Cavallini (2003) introduced an interfacial roughness factor f_i to act on the convective coefficient α_c and to account for the increase in the heat transfer coefficient due to the action of the interfacial shear between the condensate and the vapour, arguing that the vapor shear increases the magnitude and number of the waves generated on the interface, tending to increase heat transfer. The same correction factor acting on α_c is applied to the vapor heat transfer coefficient in the above

expression, where f_i is computed from [8.1.40] or [8.1.41]. The vapor heat transfer coefficient α_G is computed with the Dittus and Boelter (1930) equation:

$$\alpha_G = 0.023\left(\frac{k_G}{d_i}\right)Re_G^{0.8}\,Pr_G^{0.33} \qquad [8.3.6]$$

using the following expression for the Reynolds number of the vapor phase and u_G from [8.1.37]:

$$Re_G = \frac{\rho_G u_G d_i}{\mu_G} \qquad [8.3.7]$$

Thus, the new approach calculates the vapor heat transfer coefficient from the actual vapor velocity rather assuming the vapor occupies the entire cross-section of the channel.

The Silver-Bell-Ghaly procedure is applied to the film condensation component as in [8.3.4] to [8.3.7] but with $F_i = 1.0$ since it was assumed in the original pure fluid model that there were no waves on the falling condensation film. The film condensation heat transfer coefficient of the zeotropic mixture in a stratified type of flow is a function of the saturation to wall temperature difference and this effect is incorporated in the expression for α_{fm} as follows:

$$\alpha_{fm} = F_m\left[\frac{1}{\alpha_f} + R_c\right]^{-1} \qquad [8.3.8]$$

In this expression, α_f is calculated with mixture properties and R_c from [8.3.5] with $F_i = 1.0$. The non-equilibrium mixture factor F_m added to this expression accounts for non-equilibrium effects in stratified flow regimes, which was correlated as follows:

$$F_m = \exp\left[-0.25(1-x)\left(\frac{\dot{m}_{wavy}}{\dot{m}}\right)^{0.5}\left(\frac{\Delta T_{glide}}{T_{sat}-T_w}\right)\right] \qquad [8.3.9]$$

Values of F_m range from 0 and 1, decreasing as the mass velocity and vapor quality decrease. The mass transfer resistance is proportional to the temperature glide and therefore F_m decreases with increasing ΔT_{glide}. The effect of the saturation to wall temperature difference is also included since it drives the mass diffusion process.

Figure 8.14 shows their entire database compared to the new mixture condensation model, plotting the ratio of the predicted values to the experimental values as a function of the temperature glide of the mixture.

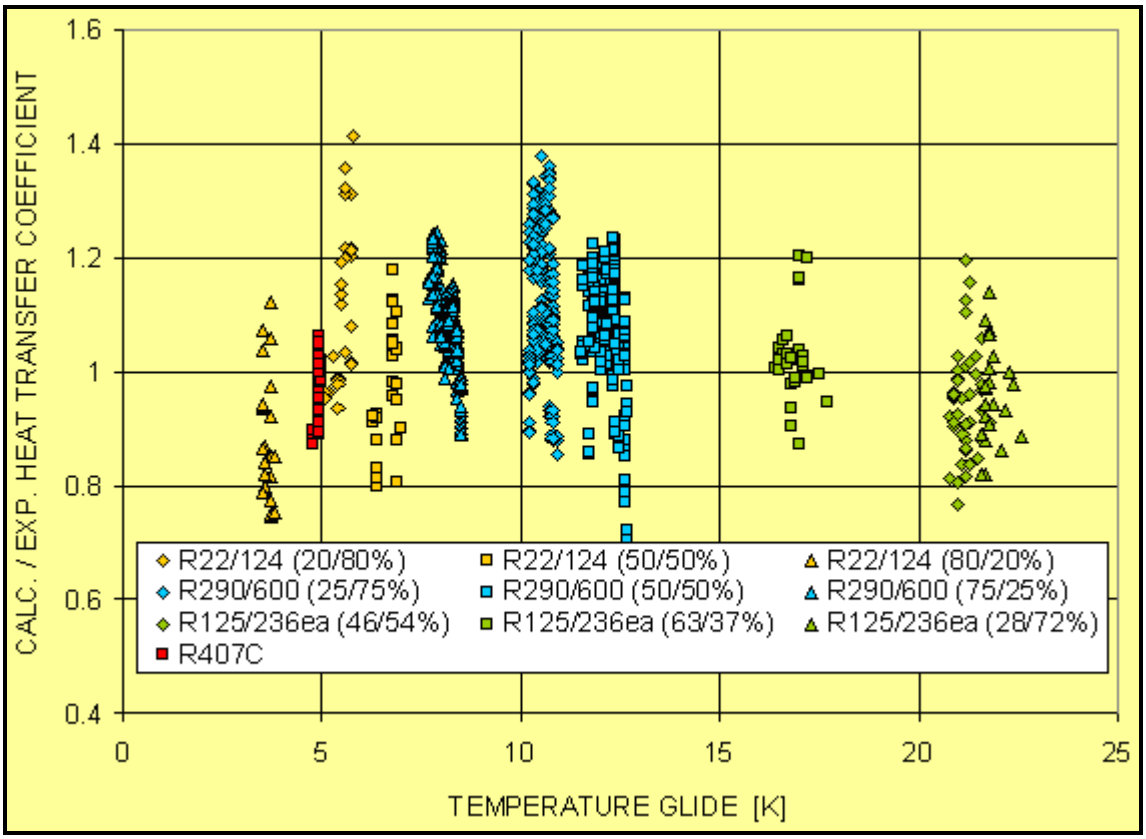

Figure 8.14. Comparison of the Del Col-Cavallini-Thome mixture condensation model to experimental data plotted versus the temperature glides of the mixtures.

Example Calculation: Propane is condensing inside a horizontal, plain tube whose internal diameter is 15 mm. The refrigerant enters at its saturation temperature of 2°C (5.07 bar) as a saturated vapor and leaves as a saturated liquid. The flow rate of vapor entering is 0.03534 kg/s and the tube wall has a mean internal temperature of -10°C. Determine the following values: the local condensing heat transfer coefficient using the Akers, Shah, and Dobson-Chato methods at a vapor quality of 0.5. Next, assuming a hydrocarbon mixture with the same physical properties as propane but with a linear temperature glide during condensation from 2°C to -3°C, determine the local condensing heat transfer coefficient using the Dobson-Chato method together with the Silver-Bell-Ghaly method at a vapor quality of 0.5. The physical properties of propane at 2°C are:

$\rho_L = 528$ kg/m^3; $\rho_G = 11.0$ kg/m^3; $\mu_L = 0.0001345$ Ns/m^2; $\mu_G = 0.0000075$ Ns/m^2;
$h_{LG} = 373100$ J/kg; $\lambda_L = 0.108$ W/m K; $c_{pL} = 2470$ J/kg K; $p_{crit} = 4264$ kPa;
$Pr_L = c_{pL}\mu_L/\lambda_L = 3.08$; $\lambda_G = 0.0159$ W/m K; $c_{pG} = 1880$ J/kg K so that $Pr_G = 0.887$.

Solution: The mass velocity of the total flow of liquid plus vapor is:

$$\dot{m} = \frac{\dot{M}}{\pi D^2/4} = \frac{0.03534}{\pi(0.015)^2/4} = 200 \text{ kg/m}^2\text{s}$$

From [5.8.5], the equivalent Reynolds number of Akers et al. (1959) is:

$$\dot{m}_e = 200\left[(1-0.5)+0.5\left(\frac{528}{11}\right)^{1/2}\right] = 792.8 \text{ kg/m}^2\text{ s}$$

so that the equivalent Reynolds number is:

$$\text{Re}_e = \frac{\dot{m}_e D}{\mu_L} = \frac{792.8(0.015)}{0.0001345} = 88416$$

For Re_e > 50,000, C = 0.0265 and n = 0.8. Applying [8.1.4], the local condensing heat transfer coefficient of Akers is:

$$\frac{\alpha(x)\,(0.015)}{0.108} = 0.0265(88416)^{0.8}(3.08)^{1/3}$$
$$\alpha(x) = 2516 \text{ W/m}^2\text{K}$$

Turning to the Shah method, the reduced pressure is 0.1189 and the liquid Reynolds number is:

$$\text{Re}_L = \frac{\dot{m} D}{\mu_L} = \frac{200(0.015)}{0.0001345} = 22305$$

Using [8.1.6], the local condensing heat transfer coefficient is:

$$\frac{\alpha(x)\,(0.015)}{0.108} = 0.023(22305)^{0.8}(3.08)^{0.4}\left[(1-0.5)^{0.8} + \frac{3.8(0.5)^{0.76}(1-0.5)^{0.04}}{(0.1189)^{0.38}}\right]$$
$$\alpha(x) = 4283 \text{ W/m}^2\text{K}$$

The Dobson and Chato method is implemented as follows. The three dimensionless groups are calculated from [8.1.9], [8.1.10] and [8.1.14]:

$$\text{Re}_{Ls} = \frac{200(0.015)(1-0.5)}{0.0001345} = 11152$$

$$X_{tt} = \left(\frac{1-0.5}{0.5}\right)^{0.9}\left(\frac{11}{528}\right)^{0.5}\left(\frac{0.0001345}{0.0000075}\right)^{0.1} = 0.1926$$

$$\text{Ga}_L = \frac{9.81(528)(528-11)(0.015)^3}{(0.0001345)^2} = 499600000$$

The transition criterion is obtained from [8.1.20]:

$$\text{Fr}_{so} = 0.025(11152)^{1.59}\left(\frac{1+1.09(0.1926)^{0.039}}{0.1926}\right)^{1.5}\frac{1}{(499600000)^{0.5}} = 103.7$$

When $Fr_{so} > 20$, the annular flow correlation [8.1.7] is used:

$$Nu(x) = 0.023(11152)^{0.8}(3.08)^{0.4}\left[1 + \frac{2.22}{(0.1926)^{0.89}}\right] = 662.2$$

From [8.1.8], the local condensing coefficient is obtained:

$$Nu(x) = \frac{\alpha(x)(0.015)}{0.108} = 662.2$$
$$\alpha(x) = 4768 \text{ W/m}^2\text{K}$$

Thus, the methods of Akers, Shah and Dobson-Chato give the respective values of 2516, 4283 and 4768 W/m^2 K. The fall in the dew point temperature over the entire condensation range is 5°C (= dT_{dew}). The total enthalpy change is that of the latent heat plus sensible heat. The latter can be estimated as the mean of the liquid and vapor specific heats applied to the condensing temperature glide of 5°C. Thus, dh = (1/2)(2470+1880)(5) + 373100 = 10875 + 373100 = 383975 J/kg. Applying [8.3.2] gives:

$$Z_G = 0.5(1880)\frac{5}{383975} = 0.01224$$

The Reynolds number of the vapor fraction is:

$$Re_{Gs} = \frac{200(0.015)(1-0.5)}{0.0000075} = 200000$$

The convection heat transfer coefficient to the vapor is obtained with the Dittus-Boelter single-phase turbulent flow correlation:

$$\frac{\alpha_G(0.015)}{0.0159} = 0.023(200000)^{0.8}(0.887)^{0.4}$$
$$\alpha_G = 404.6 \text{ W/m}^2\text{K}$$

Applying [8.3.1] gives the condensing coefficient of the mixture as:

$$\frac{1}{\alpha_{eff}} = \frac{1}{4768} + \frac{0.01224}{404.6}$$
$$\alpha_{eff} = 4160 \text{ W/m}^2\text{K}$$

The mass transfer effect reduces the condensing heat transfer coefficient by 13% for these conditions.

8.4 Condensation of Superheated Vapor

Cooling of superheated vapors involves condensation when the wall temperature is below the saturation temperature of the vapor, or one of its components if a mixture. In order to determine if condensation

occurs, a step-wise calculation of the wall temperature must be performed, using the cooling fluid's heat transfer coefficient and the single-phase heat transfer coefficient of the vapor phase in the thermal resistance analysis. The temperatures of the hot and cold fluids change along the flow path of the superheated vapor and the local values are used to calculate the wall temperature on the vapor-side. If the wall temperature goes below the saturation temperature, then condensation of the superheated vapor will occur in the thermal boundary layer on the tube wall, even though the bulk vapor is superheated. Since condensing heat transfer is much more effective than single-phase heat transfer to a vapor, it is imperative to include this effect in the thermal design of the condenser if this zone is significant with respect to the saturated condensing zone. To estimate the condensing heat transfer coefficient in this desuperheating zone, it is common practice to use the same thermal design equation as in the saturated zone. The saturated zone method should normally be evaluated at a vapor quality of 0.99 and not at 1.0 since some of these methods will "crash" at a vapor quality of 1.0 or go to the single-phase turbulent flow heat transfer coefficient.

The above scenario is based on the assumption that the process reached this operating state from a hot process path, for example if the superheated vapor is flowing through the heat exchanger before the coolant flow is applied. If instead the coolant is applied first to the heat exchanger, then the subsequent flow of the superheated vapor will find a wall temperature below saturation. In this case, the desuperheating zone will be found by using the condensing heat transfer coefficient in the thermal resistance analysis rather than the single-phase heat transfer coefficient of the vapor phase.

8.5 Subcooling of Condensate

Methods for predicting heat transfer and pressure drop for single-phase flow of liquids should be used for the subcooling zone of the condenser. In actual fact, the condensate may still contain some bubbles that have not yet condensed (remember this is a dynamic process and not an equilibrium thermodynamic process) but their effect on thermal performance will not be significant. The flow may be either laminar or turbulent. Also, for internally enhanced tubes, an appropriate method for the particular enhancement operating in the single-phase mode should be used. For example, for microfin tubes the methods for predicting heat transfer and pressure drop inside internally ribbed tubes should be used.